Electronic Supplementary Material (ESI) for Journal of Materials Chemistry B.

Nitrogen-doped graphene quantum dot-based portable fluorescence sensor for the sensitive detection of Fe^{3+} and ATP with logic gate operation

Hongyuan Zhang[a,b], Jieqiong Wang[a,b], Shanshan Wei[a,b], Chenzhao Wang[a,b], Xiangyu Yin[a,b], Xuewei Song[a,b], Chunzhu Jiang[a] and Guoying Sun[a,b,]*

[a]*School of Chemistry and Life Science, Changchun University of Technology, 2055 Yanan Street, Changchun 130012, P. R. China.*

[b]*Advanced Institute of Materials Science, Changchun University of Technology, 2055 Yanan Street, Changchun 130012, P. R. China.*

Reagents and Instrument

Graphite powder, P_2O_5, H_2SO_4, $K_2S_2O_8$, HCl, $KMnO_4$, N, N-dimethylformamide (DMF), adenosine triphosphate (ATP), Uridine triphosphate (UTP), guanosine triphosphate (GTP), cytidine triphosphate (CTP), Adenosine monophosphate (AMP), and adenosine diphosphate (ADP), $FeCl_3$, NaCl, LiCl, KCl, $CaCl_2$, AgCl, $PbCl_2$, $ZnCl_2$, $MnCl_2$, $BaCl_2$, $CdCl_2$, $AlCl_3$ were provided by Aladdin (China). Lysine (Lys), tyrosine (Tyr), histidine (His), arginine (Arg),and glucose (Glu), were bought from Macklin (China). 4T1 cells (mouse breast cancer cells) were provided by the Chinese National Cell Line Resource Infrastructure. Ultrapure water prepared by Milli-Q Gradient ultrapure water system (Millipore) was used throughout the experiments.

Instrument

The morphological and crystallographic characteristics of the materials were investigated by high-resolution transmission electron microscope (HR-TEM) (JEOL-2100F). UV-Vis spectra were measured on a spectrophotometer (Varian Cary 50). Fourier transform infrared spectroscopy (FT-IR) measurements were carried out using Is50 (PerkinElmer, USA). Raman spectra were used to analyze the structure information of the as-obtained samples (LABRAM HR Evolution). X-ray diffraction (XRD) patterns of the samples were measured using Cu K_α radiation (RIGAKU D MAX 2500). X-ray photoelectron spectroscopy (XPS) was performed using monochromated Al K_α radiation as an X-ray source (A VG ESCALAB MKII spectrometer). Fluorescence excitation and emission spectra were collected with a fluorescence spectrometer (PerkinElmer LS-55). All photographs of cells were captured by an inverted fluorescence microscope (DMI4000B, Leica). The absolute photoluminescence quantum yield (Φ) was measured with QuantaMaster 8000 fluorescence spectrometer.

Preparation of Graphene Oxide

Graphene oxide (GO) was synthesized from graphitic power according to modified Hummer's method. Briefly, 0.75 g graphite powder was added into a solution consisting of 4.5 mL concentrated H_2SO_4, 1.125 g $K_2S_2O_8$, and 1.125 g P_2O_5 and reacted at 80 °C for 5 h[1]. After cooling to room temperature, 100 mL of ultrapure water was slowly added. The product was filtered by 0.2 μm Nylon film and dried naturally. Pretreated graphite powder was further oxidized by 20 mL H_2O_2 (30%) and10 g $KMnO_4$ at 38°C for 5h[2]. After that, the reaction was ended with the addition of 200 mL deionized water, and 20 mL H_2O_2 (30%). In the end, the mixture was washed 3 times with 1: 10 (v: v) HCl aqueous solution, and then deionized water[3]. Finally, GO was exfoliated by sonicating for 2 h under ice bath. The GO solid was obtained by removing the aqueous medium with a vacuum freeze drier.

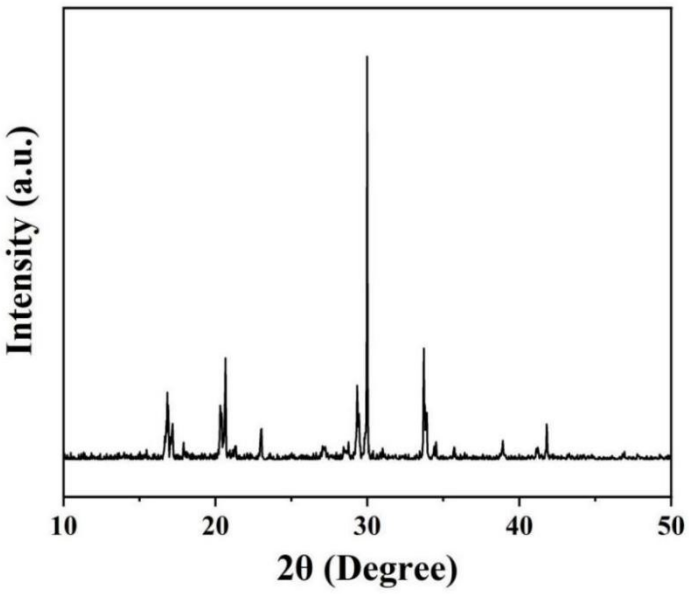

Figure S1 X-ray diffraction pattern of N-GQDs.

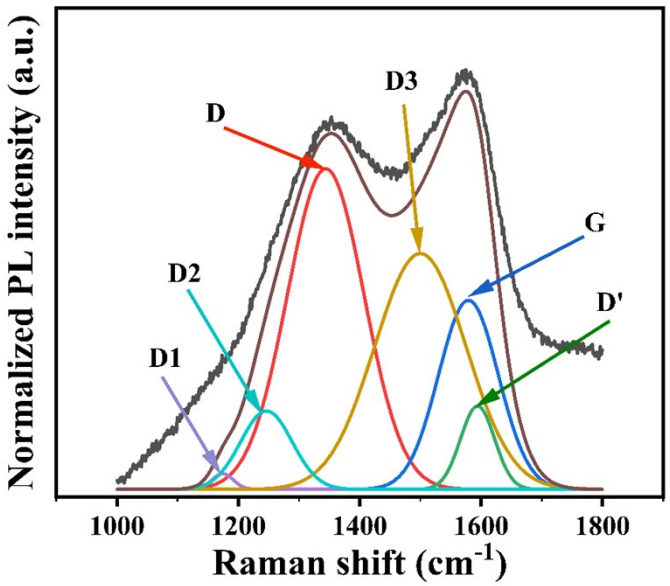

Figure S2 Fitted curves of Gaussian peaks (D1, D2 and D3) and Lorentzian peaks (D, G and D') of N-GQDs Raman spectra.

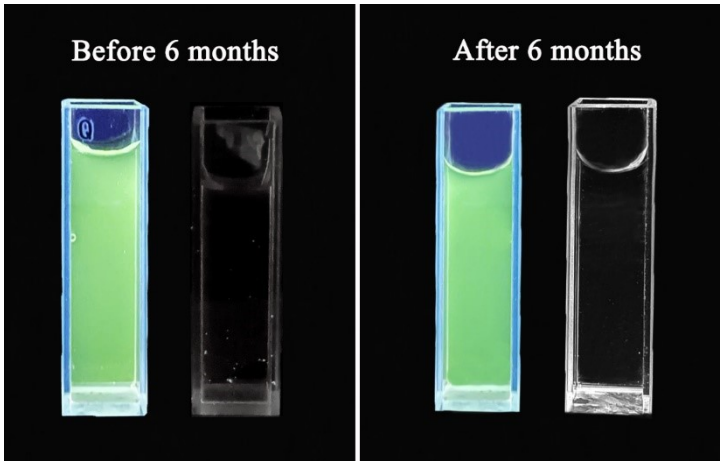

Figure S3 Shelf-life assessment of the sensor

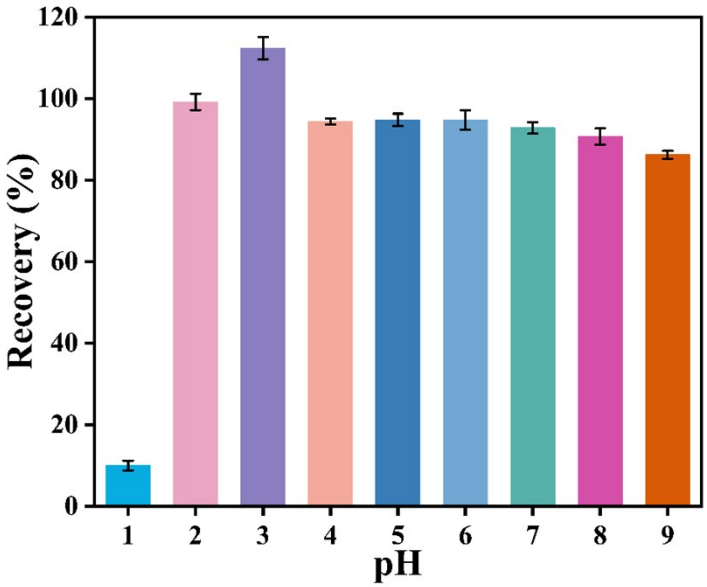

Figure S4 Fluorescence stability studies of N-GQDs for sensing Fe^{3+} in different pH solutions.

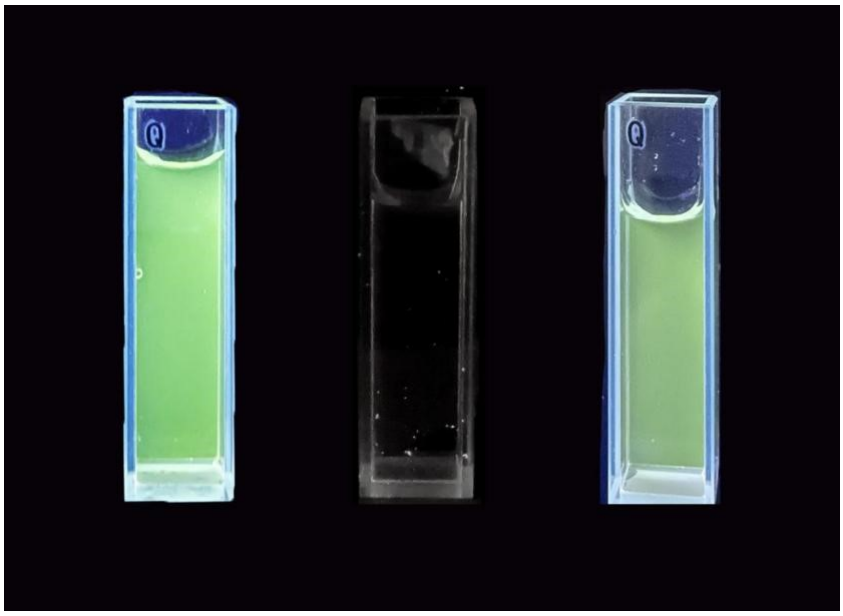

Figure S5 “ON-OFF-ON” process under UV lamp.

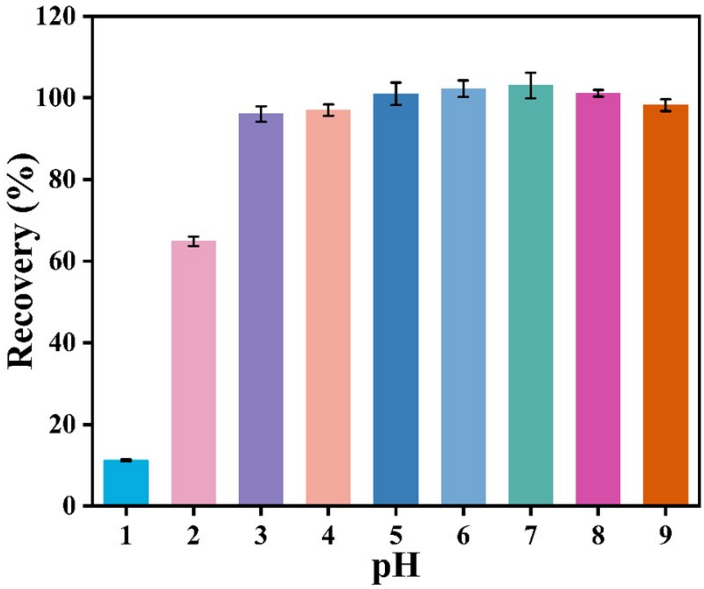

Figure S6 Fluorescence stability studies of N-GQDs-Fe^{3+} system for sensing ATP in different pH solutions.

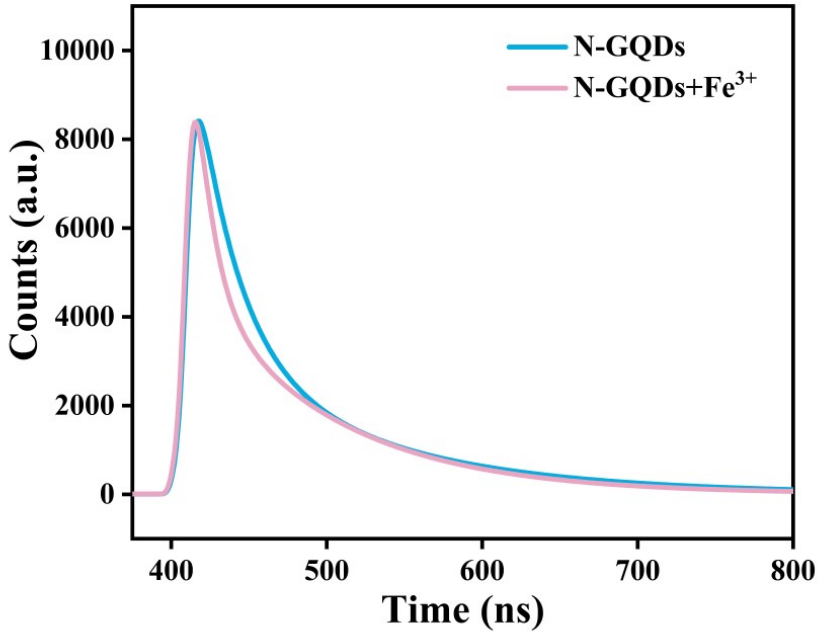

Figure S7 Time-resolved fluorescence of N-GQDs.

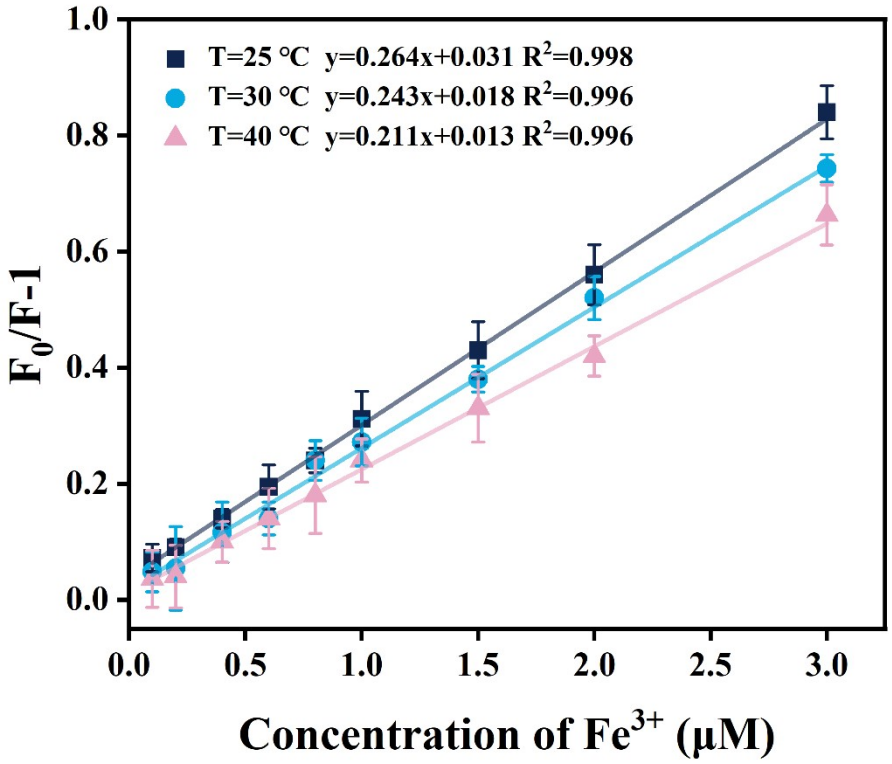

Figure S8 Stern-Vlomer linear fitting for the fluorescence quenching of N-GQDs at different temperatures in the presence of Fe^{3+}

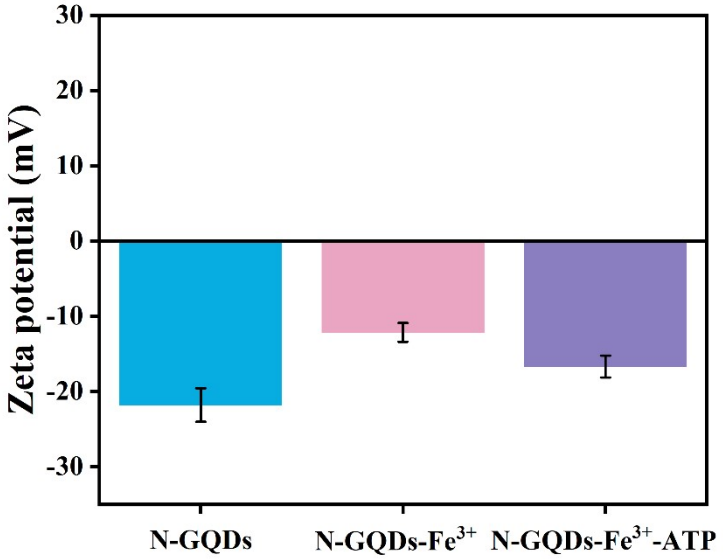

Figure S9 Zeta potentials of N-GQDs, N-GQDs-Fe^{3+} system and N-GQDs-Fe^{3+}-ATP system

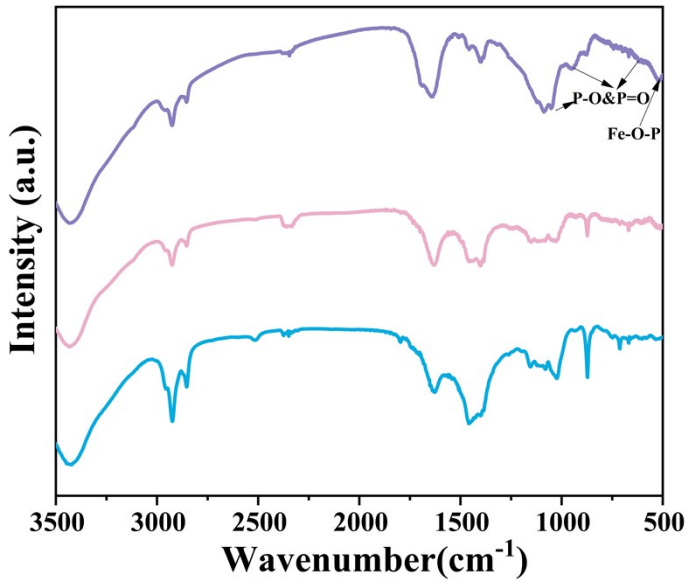

Figure S10 FT-IR spectra and their characteristic vibrational modes, where the blue line was for N-GQDs, the pink line was for the N-GQDs-Fe^{3+} system, and the purple line was for the N-GQDs-Fe^{3+}-ATP system.

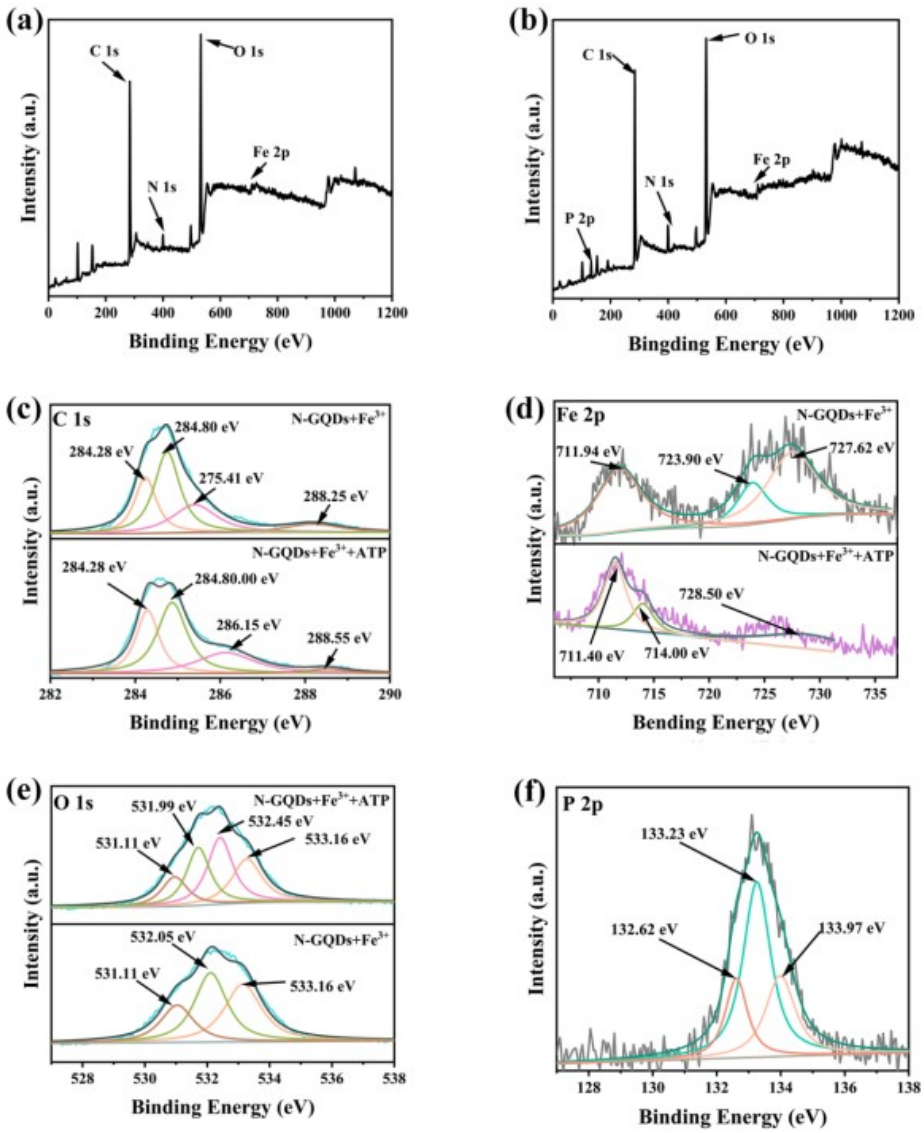

Figure S11.(a) XPS full spectrum of N-GQDs-Fe^{3+} system; (b) XPS full spectrum of N-GQDs-Fe^{3+} system; (c) C1s XPS spectra of N-GQDs-Fe^{3+} system and N-GQDs-Fe^{3+}-ATP system; (d) P2p XPS spectra of N-GQDs-Fe^{3+}-ATP system; (e) Comparison of O1s XPS spectra of N-GQDs-Fe^{3+} and N-GQDs-Fe^{3+}-ATP system; (f) Fe 2P1/2 and Fe 2P3/2 XPS spectra of N-GQDs-Fe^{3+} and N-GQDs-Fe^{3+}-ATP systems, with satellite peaks indicated by orange.

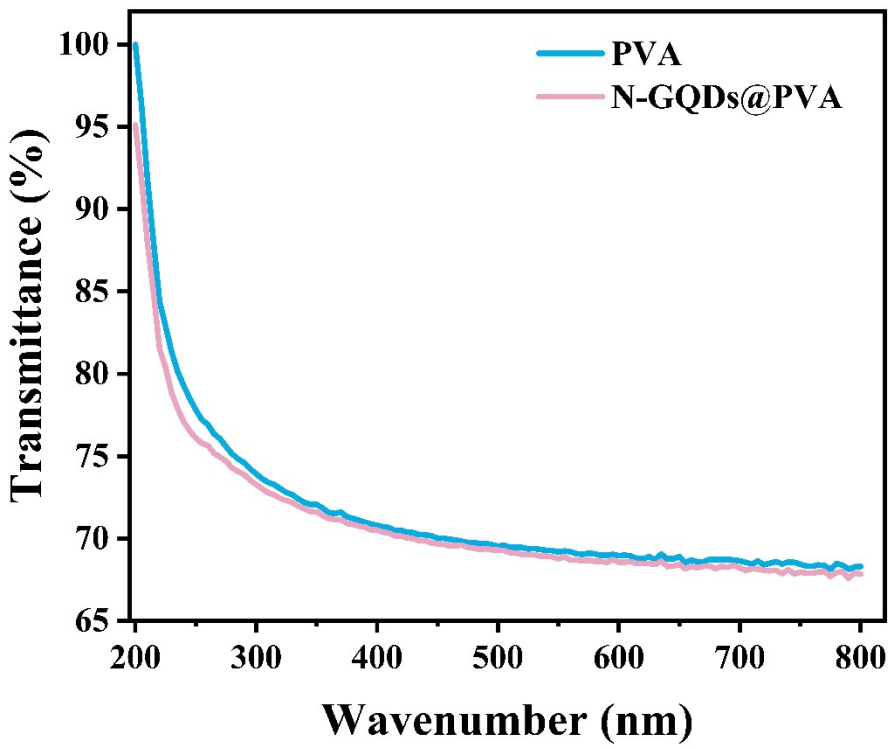

Figure S12 UV spectral transmission tests of pure PVA films and fluorescent flexible films mixed with N-GQDs.

Table.S1 Comparison of different sensors for the Sensing of Fe^{3+}

Type of sensor	linear range (μM)	LODs (nM)	Ref.
GB-CDs	50.00-600.00	60.00	4
N-GQDs	1.00-70.00	80.00	5
N-CDs	5.00-60.00	1900.00	6
Mn, B, N-CDs	0-800.00	780.00	7
S-CDs	1.00-500.00	100.00	8
N-GQDs	10.00-1000.00	190.00	9
MXene quantum dots	5.00-1000.00	310.00	10
AMHMPQ	1000.00-15000.00	962.60	11
Ag-MOF	0–575.00	15440.00	12
N-GQDs	0-34.05	2.38	This work

Table.S2 Comparison of other works for the detection of ATP

Type of sensor	linear range (μM)	LODs (nM)	Ref.
AgNCs	0.01-18.00	8.40	[13]
DNA-F	20.00-3500.00	3200.00	[14]
TC/Apt	1.00-1500.00	200.00	[15]
Hemin/G-quadruplex	0.10-2.00	40.00	[16]
Dendritic DNA nanoassembly	10.00-10000.00	5.80	[17]
NEase	10.00-100000.00	3.40	[18]
ThT-SCD	0-150000.00	1300.00	[19]
N-GQDs	0-10.00	1.16	This work

Table. S3 Determination of Fe^{3+} and ATP in actual samples

Fe^{3+}	Added (nM)	Founded (nM)	Recovery (%)	RSDs (%) (n=3)	ATP	Added (nM)	Founded (nM)	Recovery (%)	RSDs (%) (n=3)
Mice serum	0	-	-	0.12	Mice serum	0	-	-	0.17
	100	100.23	100.23	1.12		100	100.62	100.62	2.25
	200	196.06	98.03	1.35		200	199.54	99.77	1.61
	500	505.91	101.18	0.56		500	510.50	102.10	2.42
urine	0	-	-	1.22	urine	0	-	-	1.46
	100	99.50	99.50	2.71		100	96.90	96.90	0.25
	200	201.04	100.52	0.83		200	214.24	107.12	2.49
	500	522.93	104.59	1.42		500	562.12	112.42	1.36

Table S4 Intra-day and Inter-day precision tests

	matrix	Added (nM)	Intra-day precision (%) (n=3)	Inter-day precision (%) (n=6)
Fe^{3+}	mice serum	100	100.21±1.24	99.79±3.72
		200	101.37±1.34	95.52±2.64
		500	99.64±0.72	99.55±3.11
	urine	100	105.50±1.76	100.10±1.73
		200	100.16±1.40	104.38±4.68
		500	108.46±2.41	103.64±3.26
ATP	mice serum	100	98.19±2.79	95.45±4.83
		200	107.96±0.41	99.53±4.93
		500	99.80±1.16	100.21±2.69
	urine	100	102.30±1.80	99.11±4.97
		200	105.35±0.37	102.20±5.55
		500	102.76±1.37	95.80±5.31

References:

1. Zhu, Y.; Kong, G.; Pan, Y.; Liu, L.; Yang, B.; Zhang, S.; Lai, D.; Che, C., An improved Hummers method to synthesize graphene oxide using much less concentrated sulfuric acid. *Chinese Chemical Letters* **2022,** *33* (10), 4541-4544.
2. Wang, Y.; Li, Z.; Hu, D.; Lin, C.-T.; Li, J.; Lin, Y., Aptamer/Graphene Oxide Nanocomplex for in Situ Molecular Probing in Living Cells. *Journal of the American Chemical Society* **2010,** *132* (27), 9274-9276.
3. Marcano, D. C.; Kosynkin, D. V.; Berlin, J. M.; Sinitskii, A.; Sun, Z.; Slesarev, A. S.; Alemany, L. B.; Lu, W.; Tour, J. M., Correction to Improved Synthesis of Graphene Oxide. *ACS Nano* **2018,** *12* (2), 2078-2078.
4. Durrani, S.; Zhang, J.; Mukramin; Wang, H.; Wang, Z.; Khan, L. U.; Zhang, F.; Durrani, F.; Wu, F.-G.; Lin, F., Biomass-Based Carbon Dots for Fe3+ and Adenosine Triphosphate Detection in Mitochondria. *ACS Applied Nano Materials* **2023,** *6* (1), 76-85.
5. Xu, H.; Zhou, S.; Xiao, L.; Wang, H.; Li, S.; Yuan, Q., Fabrication of a nitrogen-doped graphene quantum dot from MOF-derived porous carbon and its application for highly selective fluorescence detection of Fe3+. *Journal of Materials Chemistry C* **2015,** *3* (2), 291-297.
6. Cui, J.; Zhu, X.; Liu, Y.; Liang, L.; Peng, Y.; Wu, S.; Zhao, Y., N-Doped Carbon Dots as Fluorescent "Turn-Off" Nanosensors for Ascorbic Acid and Fe3+ Detection. *ACS Applied Nano Materials* **2022,** *5* (5), 7268-7277.

7. Li, B.; Xiao, X.; Hu, M.; Wang, Y.; Wang, Y.; Yan, X.; Huang, Z.; Servati, P.; Huang, L.; Tang, J., Mn, B, N co-doped graphene quantum dots for fluorescence sensing and biological imaging. *Arabian Journal of Chemistry* **2022,** *15* (7), 103856.

8. Xu, Q.; Pu, P.; Zhao, J.; Dong, C.; Gao, C.; Chen, Y.; Chen, J.; Liu, Y.; Zhou, H., Preparation of highly photoluminescent sulfur-doped carbon dots for Fe(iii) detection. *Journal of Materials Chemistry A* **2015,** *3* (2), 542-546.

9. Yang, F.; Bao, W.; Liu, T.; Zhang, B.; Huang, S.; Yang, W.; Li, Y.; Li, N.; Wang, C.; Pan, C.; Li, Y., Nitrogen-doped graphene quantum dots prepared by electrolysis of nitrogen-doped nanomesh graphene for the fluorometric determination of ferric ions. *Microchimica Acta* **2020,** *187* (6), 322.

10. Zhang, Q.; Sun, Y.; Liu, M.; Liu, Y., Selective detection of Fe3+ ions based on fluorescence MXene quantum dots via a mechanism integrating electron transfer and inner filter effect. *Nanoscale* **2020,** *12* (3), 1826-1832.

11. Mohan, B.; Xing, T.; Kumar, S.; Kumar, S.; Ma, S.; Sun, F.; Xing, D.; Ren, P., A chemosensing approach for the colorimetric and spectroscopic detection of Cr3+, Cu2+, Fe3+, and Gd3+ metal ions. *Science of The Total Environment* **2022,** *845*, 157242.

12. Mohan, B.; Ma, S.; Kumar, S.; Yang, Y.; Ren, P., Tactile Sensors: Hydroxyl Decorated Silver Metal–Organic Frameworks for Detecting Cr2O72–, MnO4–, Humic Acid, and Fe3+ Ions. *ACS Applied Materials & Interfaces* **2023,** *15* (13), 17317-17323.

13. Chen, C.; Zhao, D.; Jiang, Y.; Ni, P.; Zhang, C.; Wang, B.; Yang, F.; Lu, Y.; Sun, J., Logically Regulating Peroxidase-Like Activity of Gold Nanoclusters for Sensing Phosphate-Containing Metabolites and Alkaline Phosphatase Activity. *Analytical Chemistry* **2019,** *91* (23), 15017-15024.

14. Liu, Z.; Zhong, Y.; Hu, Y.; Yuan, L.; Luo, R.; Chen, D.; Wu, M.; Huang, H.; Li, Y., Fluorescence strategy for sensitive detection of adenosine triphosphate in terms of evaluating meat freshness. *Food Chemistry* **2019,** *270*, 573-578.

15. Chu, B.; Wang, A.; Cheng, L.; Chen, R.; Shi, H.; Song, B.; Dong, F.; Wang, H.; He, Y., Ex vivo and in vivo fluorescence detection and imaging of adenosine triphosphate. *Journal of Nanobiotechnology* **2021,** *19* (1), 187.

16. Wei, J.; Li, Y.; Si, Q.; Xiao, Q.; Chen, Q.; Jiao, T.; Chen, Q.; Chen, X., Hemin/G-quadruplex based electrochemical sensor for highly sensitive detection of ATP in fish. *Journal of Electroanalytical Chemistry* **2022,** *916*, 116374.

17. Ding, X.; Wang, Y.; Cheng, W.; Mo, F.; Sang, Y.; Xu, L.; Ding, S., Aptamer based electrochemical adenosine triphosphate assay based on a target-induced dendritic DNA nanoassembly. *Microchimica Acta* **2017,** *184* (2), 431-438.

18. Hu, T.; Wen, W.; Zhang, X.; Wang, S., Nicking endonuclease-assisted recycling of target–aptamer complex for sensitive electrochemical detection of adenosine triphosphate. *Analyst* **2016,** *141* (4), 1506-1511.

19. Singh, V. R.; Singh, P. K., A supramolecule based fluorescence turn-on and ratiometric sensor for ATP in aqueous solution. *Journal of Materials Chemistry B* **2020,** *8* (6), 1182-1190.